Digest Journal of Nanomaterials and Biostructures Vol. 11, No. 3, July – September 2016, p. 795 - 803

PSEUDOCAPACITIVE FEATURES OF CuO NANOWORMS AND Mn DOPED CuO NANOFLAKES AND THEIR PROSPECTS AS ELECTRODE MATERIALS FOR SUPERCAPACITORS

R. SURESH[a*], K. TAMILARASAN[b], D. S.VADIVU[c]
[a]*Department of Physics, Sri Eshwar College of Engineering, Kondampatti, Kinathukadavu, Coimbatore, Tamil Nadu, India- 641202*
[b]*Department of Physics, Kongu Engineering College, Erode, Tamilnadu, India- 638 052*
[c]*Departments of Chemistry, Dr.Mahalingam College of Engineering and Technology, Pollachi, Tamilnadu, India- 642 003*

Copper oxide (CuO) and manganese (Mn) doped CuO nanostructures have been synthesized via facile solution routeand their electrochemical properties were analysed towards supercapacitor electrode application. Morphological investigations reveals the formation of nanoworm like structure for CuO in which addition of Mn lead to the configuration of flake like morphology. Electrochemical nature of the materials were studied using cyclic voltammetric (CV), Galvanostatic charge-discharge and electrochemical impedance analysis. 5 wt% of Mn doped CuO nanoflakes exhibit the maximum specific capacitance of 625 Fg^{-1} at 2 mV s^{-1} and offers a good cyclic stability with the capacitance retention of 84% after 2000 cycles. Electrochemical impedance analysis shows a charge transfer resistance (R_{ct}) of 1 Ω for 5 wt% of Mn doped CuO nanoflakes, which is quite beneficial for better charge-discharge performance at higher current rates. These findings suggest thatMn blended CuO nanostructures prepared through cost effective and simple chemical precipitation method offers better electrochemical features.

(Recieved June 12, 2016; Accepted August 1, 2016)

*Keywords:*Nanostructures, supercapacitor,energy storage, aqueous electrolyte

1. Introduction

Increasing energy demand and growing ecological concerns are the major challenges that press the society hard to move towards efficient, low-cost and environmentally friendly energy conversion and storage systems. Currently, supercapacitors (SCs) have attracted as efficient energy storage devices due to their unique properties like high power density, superior cycle life, high durability, better efficiency, safety and environmental friendliness. SCs can complement batteries and fuel cells in various high power applications to deliver the desirable power density and energy density[1,2].

Generally, SCs possess three basic components namely, electrode, separator and an electrolyte. Among these, the electrode plays a dominant role on deciding the performance of the supercapacitor. Different materials have been exploited for SC electrode application that includes carbon based materials, conducting polymers, transition metal oxides (TMO) and hybrid materials [3-7]. Carbon materials with high surface area such as carbon nanotubes, graphene and porous carbon exhibit EDLC behavior, where charges are stored at the interface between electrode and electrolyte. The large scale application of EDLC's is limited by their low specific capacitance (100 - 200 F g^{-1}). The pseudocapacitors employ transition metal oxides (RuO_2, Co_3O_4, CuO,MnO_2, NiO) and/or conducting polymers (PANI, PPy,PEDOT) as the electrode materials due to fast reversible Faradic redox reaction, which results in 10 - 100 times higher specific capacitance than EDLC's [8-12]. However, lower electrical conductivity and structural collapse during cycling hampered the electrochemical performance of TMO[13]. Both problems should be addressed to

*Corresponding author : suresh.r@sece.ac.in

produce the commercial supercapacitors. To overcome this barrier, two strategies may be adopted (i) form mixed transition metal oxides (ii) form carbon based (CNT, graphene) hybrid composites.

For instance, Purushothaman et al., [14] synthesized CuO/rGO composite to enhance the electrochemical nature of CuO. CuO-NiO micro polyhedrons were synthesized by Zhang at al.,[15] and exploited its usefulness for supercapacitor application. When compared to pure V_2O_5, Cr doped V_2O_5 exhibits improved electrochemical performance as reported by Zhan et al., [16]. Kim et al., [17] formed Ni-NiO core shell structures and achieved better rate capacity and cyclic stability towards supercapacitor electrode applications.

Among the TMOs, cupric oxide (CuO) is an attractive material due to its characteristics like natural abundance, low cost and non-toxicity. Present work deals with the synthesis of Mn-CuO nanostructures by co- precipitation method using ethylene glycol as structural agent and disodium citrate as capping agent. Here, we address the effect of Mn doping on the structural, morphological and electrochemical properties of CuO.

2. Experimental details

2.1 Chemicals and reagents

Analytical grade $Na_2HC_6H_5O_7$(Sigma Alrich, Inc.),KOH,NaOH, (Cu $(NO_3)_2.3H_2O$ and ethylene glycol (SD Fine Chemicals Ltd., India) were used as received without further purification.

2.2 Materials synthesis

1.7728 g of copper nitrate was dissolved in 250 mL of deionised water and stirred for 10 minutes. Then, 0.0453 g of manganese nitrate was added to the solution and stirred for few minutes. Further, 2 mL of ethylene glycol and 0.09 g of disodium citrate was added to the solution followed by the addition of 2M NaOH to make the pH~ 10 and stirred for few hours to make it as a homogenous mixture. After 48 h of aging, the samples collected with the help of centrifugation were annealed at 400°C for two hours. The as-prepared samples were named as CM2.5. The amount of manganese nitrate was changed to prepare 5wt% (0.0906 g) and 7.5 wt% (0.1359 g) Mn doped samples named respectively as CM5 and CM7.5. Employing the same procedure, undoped CuO nanostructures were prepared without adding manganese nitrate.

2.3 Characterization Techniques

X-ray diffraction analysis for CuO and Mn-CuO nanostructureswere performed using PANalytical X'pert-PRO diffractometer equipped with Cu Kα sealed tube (λ = 1.5406 Å). FTIR analysis has been made using JASCO 460PLUS. The samples were scanned in the range between 10° to 80° with a step size of 0.02° and an exposure time of 10s. Field emission scanning electron microscopy (FESEM) analysis was carried out using SEM FEI-Quanta FEG 200 instrument to investigate the morphology of the samples. Energy dispersive spectra (EDS) of the samples were recorded using Bruker Quantax 200 AS instrument. Cyclic voltammetry (CV), galvanostatic charge-discharge(GCD) and electrochemical impedance spectroscopy (EIS) techniques were employed using CHI 660 D electrochemical workstation (CH Instruments) to test the supercapacitive features of the samples.

2.4 Electrode preparation

The electrode was prepared by mixing 85 wt % of active material , 10 wt % activated carbon(AC) and 5 wt % polytetrafluoroethylene (PTFE) with a few drops of ethanol. This mixture was pasted well on nickel foam surface (area = 1 cm^2) and dried at 80 °C for 4 h to get the working electrode. The electrochemical investigations were performed in a three-electrode configuration containing Ag/AgCl as reference electrode, platinum wire as counter electrode, CuO based material as working electrode and 2M KOH as electrolyte.

3. Results and discussion

3.1 Structural and morphological analysis

The crystal structure, phase and purity of the undoped CuO and Mn-CuO nanostructures were evaluated using X-ray diffraction technique. The diffraction peaks (Fig.1) obtained for the Mn-CuO samples matches well with the standard XRD pattern of CuO (JCPDS card No. 05-0661).

Corresponding to the monoclinic symmetry (C_2/C space group), these samples possess lattice parameter values of a = 4.684 A˚, b = 3.425 A˚, c = 5.129 A˚ and β = 99.47. The intensity of the diffraction peaks decreases with increase in Mn doping level. The absence of the peaks related to Mn in the XRD pattern may be attributed to the lesser doping level of Mn.

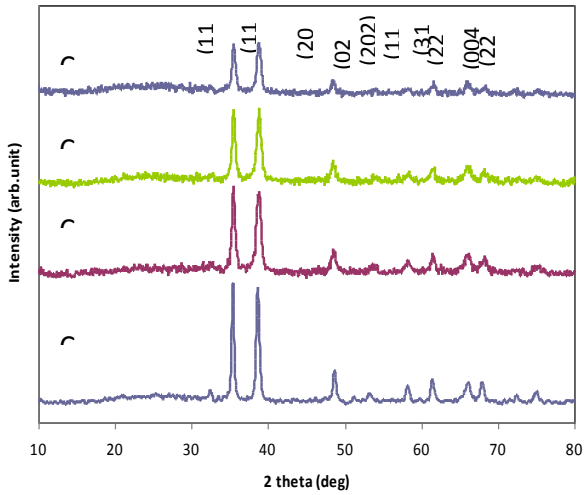

Fig. 1 XRD pattern CuO and Mn doped CuO

Fig.2.shows the FTIR spectra of CuO and Mn doped CuO samples. The bands observed around 440 and 560 cm^{-1} corresponds to stretching vibrations of Cu-O bond [18] and OH vibration of water is observed around 1640 cm^{-1}.

FESEM images of CuO and Mn doped CuO samples are presented in Fig. 3s. Nanoworm like structure has been observed for CuO , whereas 2.5 wt % and 5 wt % of Mn doped CuO samples exhibit the nanoflake like structure. Further addition of Mn (7.5wt%) leads to agglomeration of nanoflakes. An energy-dispersive X-ray spectroscope (EDS) was used to confirm the Mn content in the samples. Fig. 4 shows the EDS spectra of pure and Mn doped CuO samples which validate the existence of Mn in the CuO nanostructures with different wt% of Mn (CM2.5 : 1.55, CM5 : 3.99 and CM7.5 : 5.9).

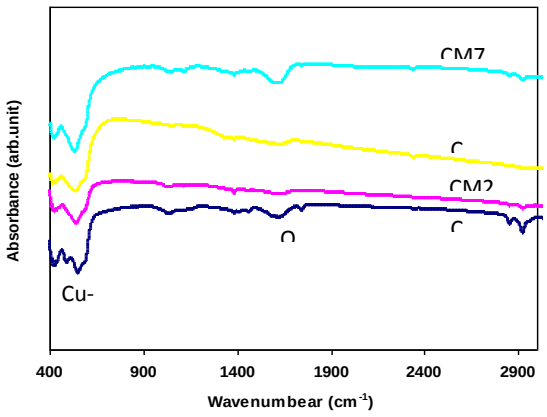

Fig.2. FTIR Spectra of CuO and Mn doped CuO

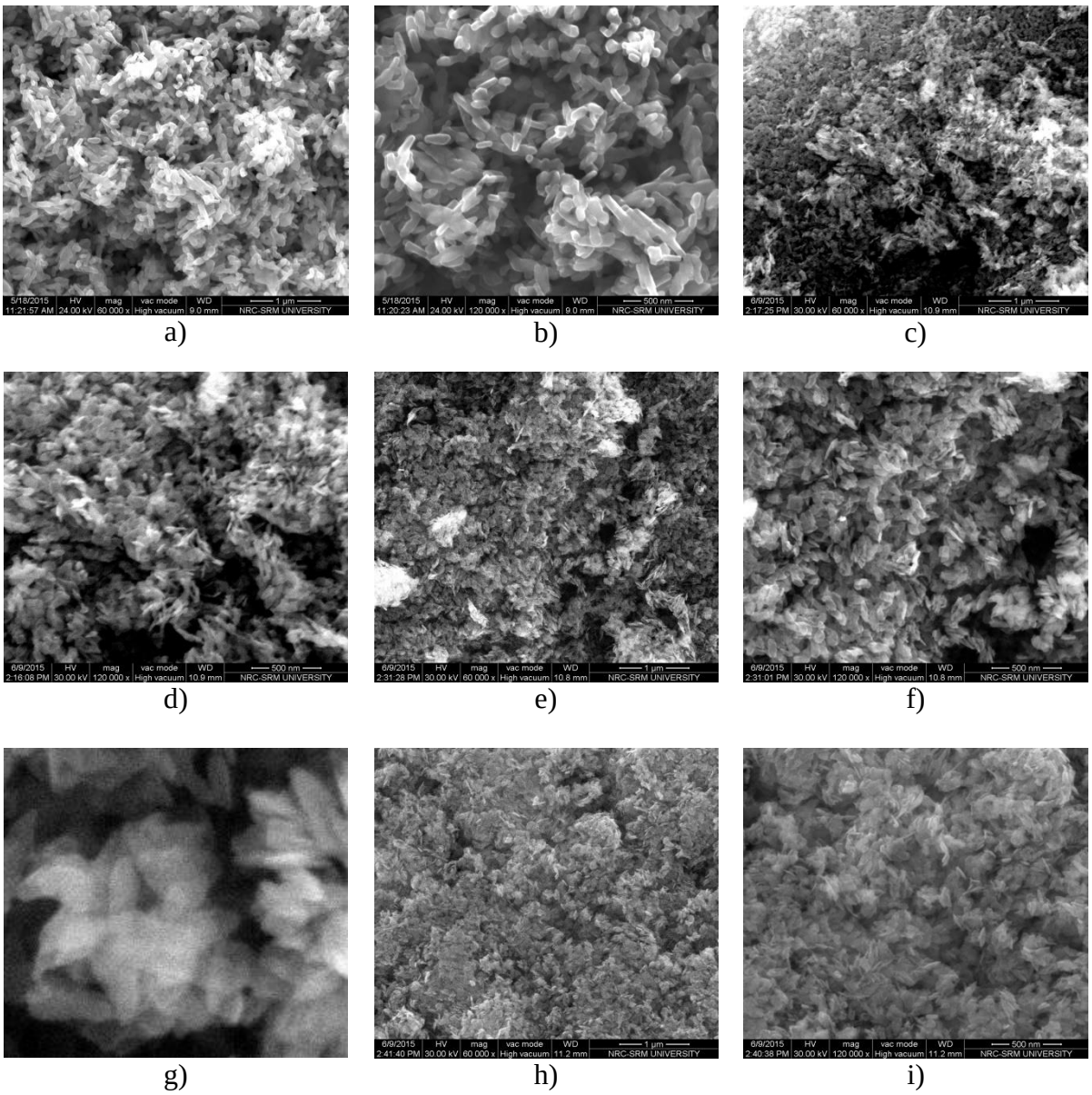

Fig. 3 SEM images of (a, b) undoped CuO, (c,d) CM2.5, (e,f,g) CM5 and (h,i) CM7.5

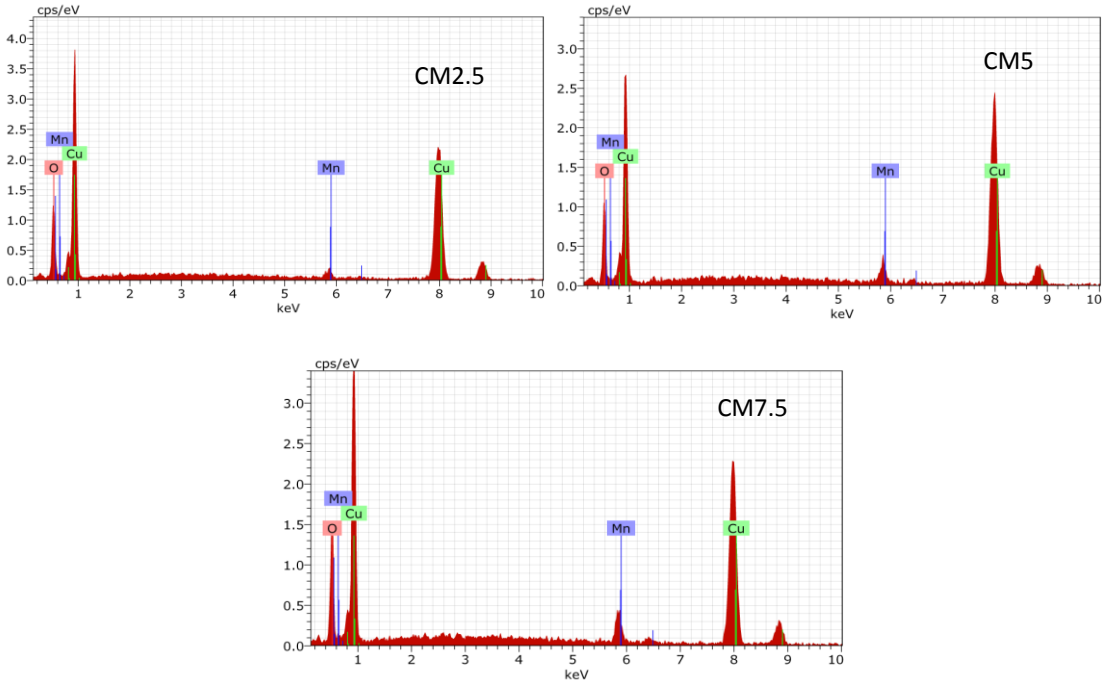

Fig.4 Energy Dispersive Spectra of pure and Mn doped CuO

3.2 Electrochemical measurements

3.2.1 Cyclic voltammetry analysis

To evaluate the energy storage behaviour, the cyclic voltammetry (CV) analysis of CuO and Mn doped CuO were carried out in a fixed potential range of 0 to 0.6 V in aqueous 2M KOH electrolyte at the scan rates from 2 to 20 mVs^{-1}. Typical CV curves forCuO, CM2.5, CM5 and CM7.5 at different scan rates are presented in Fig.5(a,b,c and d). The shape of the CV curves is different from ideal rectangular shape (due to electric double layer capacitance), indicating that the electrodes in the current work exhibit pseudo capacitance behaviour. The CV curves reveal a distinct redox peaks suggestive of the pseudocapacitive nature of CuO.

The specific capacitance of CuO and Mn blended CuO samples have been calculated from the following relation,

$$C = \frac{i}{v \times m} \tag{1}$$

where C (Fg^{-1}) is the specific capacitance, i (mA) is the average current, m (mg) is the mass of the active material and v(v) is the scan rate. The calculated specific capacitance values from CV measurements at the scan rate of 2 mVs^{-1} for CuO, CM2.5, CM5 and CM7.5 is 375 Fg^{-1}, 481Fg^{-1}, 625$Fg^{-1}$and 443Fg^{-1}respectively. It is noteworthy to mention here, the 5wt% of Mn blended sample exhibits maximum capacitance. This implies that the presence of flake like morphology in CM5 provides additional pathways for ion intercalation. Further, addition of Mn(7.5wt%) reduces the capacitance value due to stacking of flake like structures which minimizes the ion intercalation sites as presented in FESEM image. CuO-RGO composite revealed the specific capacitance of 318 Fg^{-1} at a san rate of 1 mV s^{-1} was reported by Purushothaman et al [14]. Our electrode exhibited higher value while comparing with the above work.Fig.5e shows the specific capacitance as a function of scan rate. The decrease in the specific capacitance value with the increase of scan rate proposes that the electrolyte ion does not have ample time to access the interior part of the electrode at higher scan rates. In contrast, at lower scan rates, effective penetration of ions through the surface of the active material provides higher capacitance.

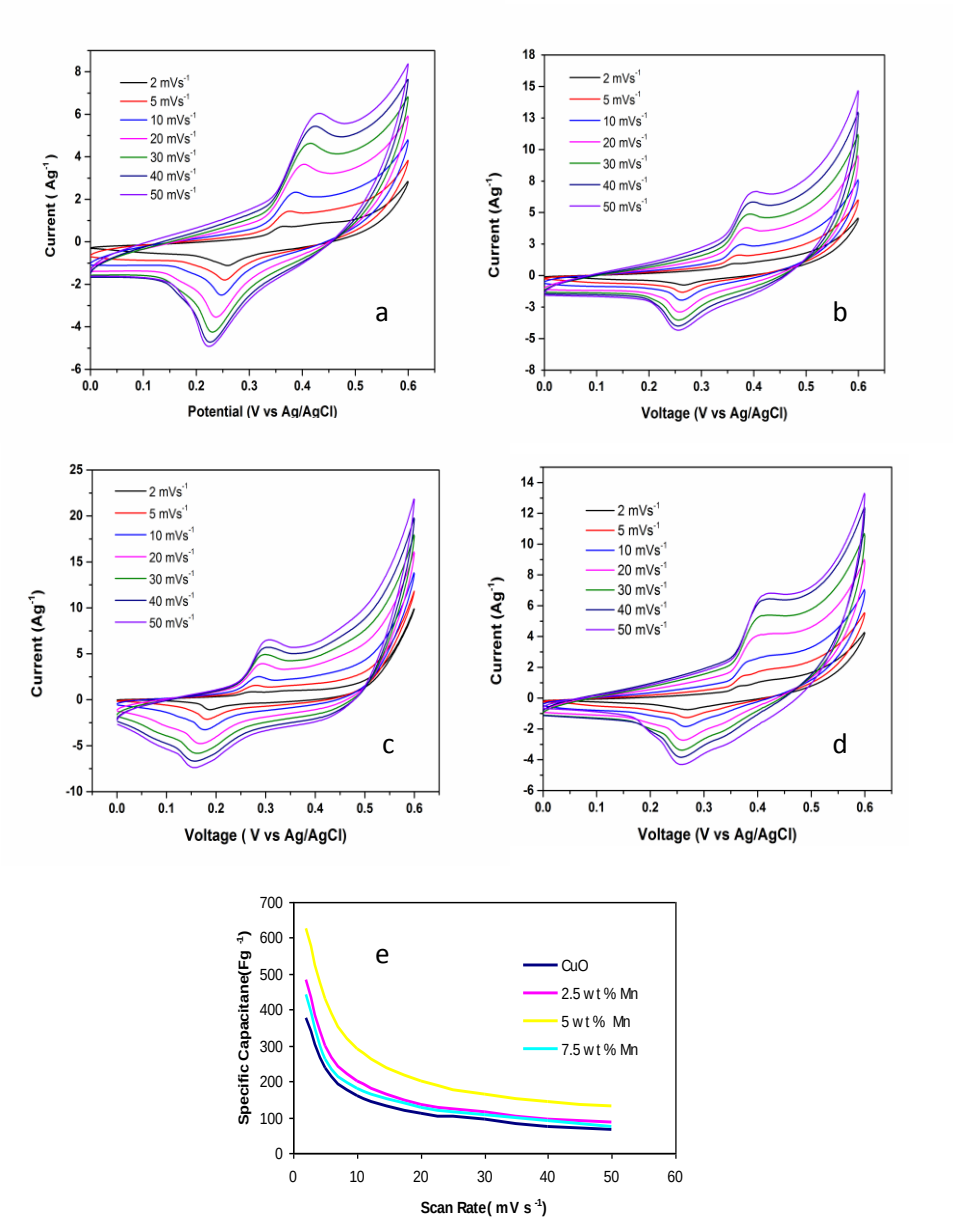

Fig.5 Cyclic voltammograms of (a) CuO, (b) 2.5wt %, (c) 5 wt % and (d) 7.5 wt % of Mn doped CuO at different scan rates, and (e) specific capacitance as a function of scan rate

3.2.2 Charge-discharge studies

To further elucidate the specific capacitance and the rate capacity, galvanostatic charge-discharge behaviour were investigated between 0 to 0.4 V at different current densities of 2 Ag^{-1}, 3 Ag^{-1}, 4 $Ag^{-1}$and 5 Ag^{-1}, and the corresponding results are presented in Fig. 6. The specific capacitance (C) has been estimated from the discharge curves according to Eq. (2),

$$C = \frac{I \times \Delta t}{m \times \Delta v} \tag{2}$$

where I (mA) is the discharge current, Δt (s) is the discharge time, Δv (V) is the potential interval of the discharge and m (mg) is the mass of the active material within the electrode. The specific capacitance of CuO, CM2.5, CM5 and CM7.5 estimated from the discharge curves are 206 Fg^{-1}, 293 Fg^{-1}, 419 Fg^{-1} and 250 Fg^{-1} respectively at 2 Ag^{-1}. As like the CV investigations, the CM5 sample exhibit higher specific capacitance when compared to other electrodes. Zhang et al[15]

reported the specific capacitance of 370 Fg^{-1} at a current density of 2 mA cm^{-1} for CuO-NiO micro polyhedrons. CuO/$Cu(OH)_2$ exhibits the specific capacitance of 278 Fg^{-1} between 0-0.55 V as reported by Hsu et al., [19]. Fig. 6b further reveals that the specific capacitance value of Mn-CuO samples strongly depends on the current density. The decrease in the specific capacitance with increasing current density is the result of the diffusion effect which restricts the migration of electrolyte ions. To evaluate the cyclic stability of the electrode materials continuous charge discharge cycles were performed ata current density of 10 Ag^{-1}. Fig. 7 shows the cyclic life of CM5. It is observed that the CM5 electrode exhibited good stability and reversibility with cycling efficiency of 84% after2000 cycles. Cu_2O microcubes exhibit the capacitance retention of 80 % after 1000 cycles was reported by Kumar et al [20]. CM5 shows better stability when compared with other works.

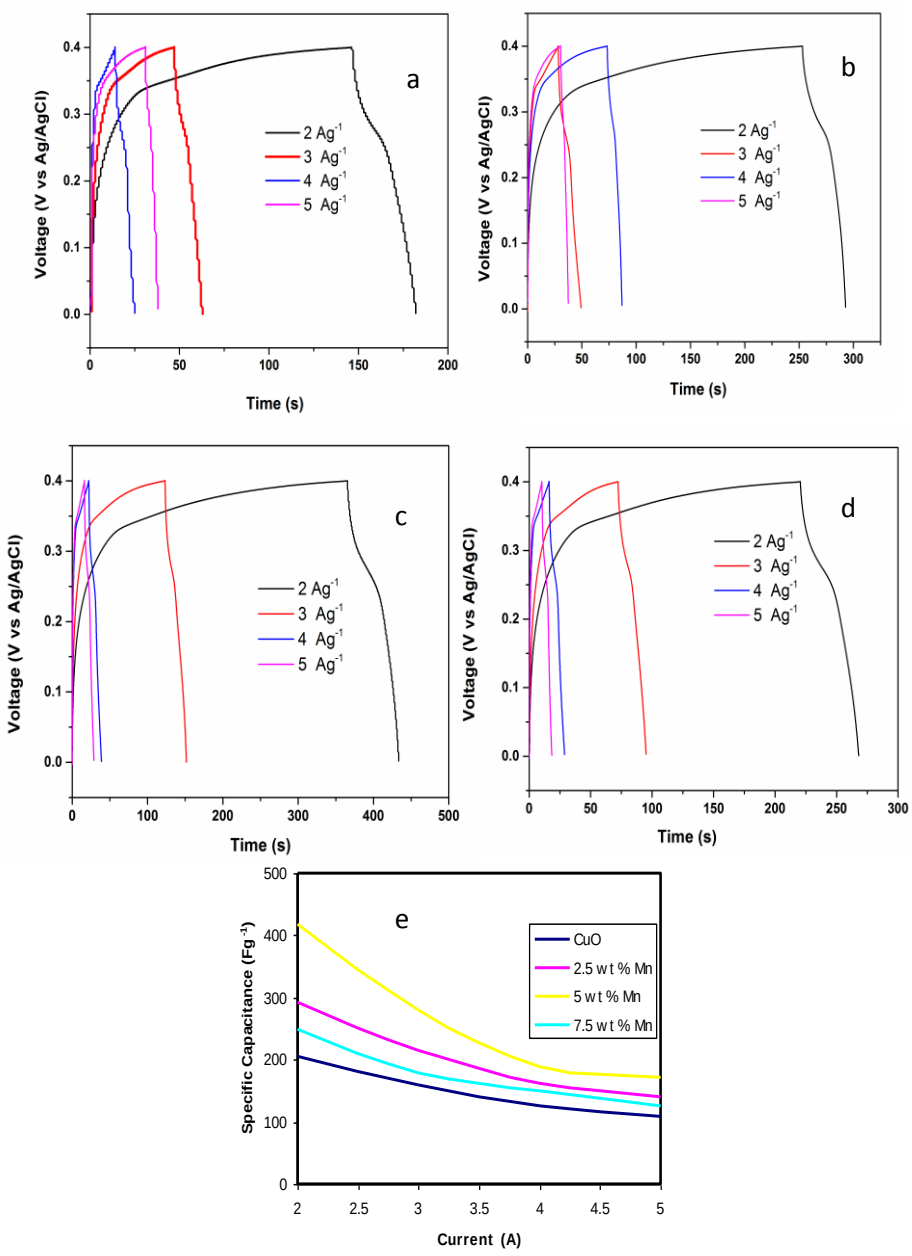

Fig. 6 GCD curves of (a) CuO (b) 2.5 wt %, (c) 5 wt % and (d) 7.5 wt % of Mn doped CuO at different current density, (e) Variation of specific capacitance with current density

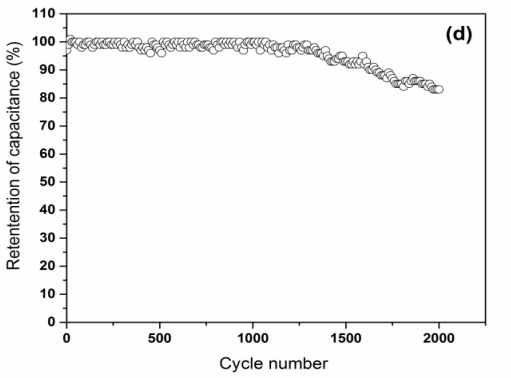

Fig.7 Cyclic Stability of CM5

3.2.3 Electrochemical impedance analysis

EIS measurements were performed on CuO and CM5 electrodes in the frequency range of 0.01 Hz - 100 kHz and the typical Nyquist plot is presented in Fig 8, which consists of a semicircle at high frequency region and a straight line at low frequency region. The semicircle present in the higher frequency range is associated with charge transfer resistance (R_{ct}) at the electrode/electrolyte interface. The R_{ct} values of CuO and CM5 electrodes is 3 Ω and 1Ω respectively. The lower R_{ct} value of CM5 electrode indicates the presence of higher number of conductive sites and results in higher specific capacitance.

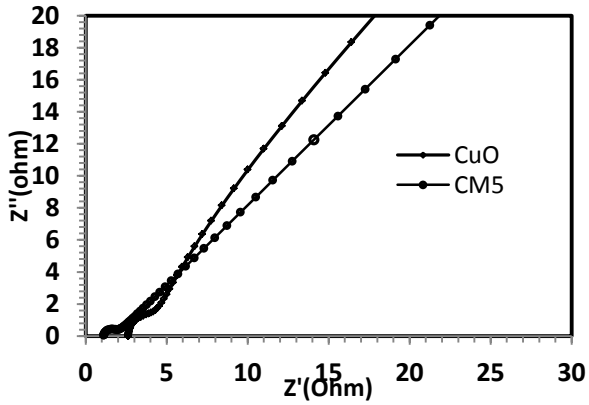

Fig. 8 Nyquist plot of CuO and CM5 electrode.

4. Conclusions

In this study, we have synthesized CuO and Mn-CuO nanostructures via chemical precipitation method for supercapacitor applications. Electrochemical measurements indicated that the 5wt% of Mn doped CuO electrode delivered a maximum specific capacitance of 625 Fg^{-1} and better cyclic stability over 2000 cycles. In addition 5wt% Mn blended CuO sample exhibits charge transfer resistance of 1Ω, which is much beneficial to perform charge-discharge at higher scan rates. These enhanced electrochemical performances coupled with the simple and low cost synthesize procedure renders Mn-CuO nanostructures as a promising candidate for applications in high-performance energy storage systems.

References

[1] P. Simon, Y. Gogotsi. Nat. Mater. **20**, 845, (2008).
[2] S. Mondal , U. Rana, S. Malik,Chem. Comm. **51**, 12365, (2015).
[3] Q. Zhao, X. Wang, H. Xia, J. Liu, H. Wang, J. Gao, Y. Zhang, J. Liu,H. Zhou, X. Li, S. Zhang, X. Wang. Electrochim Acta, **173**,566 (2015).
[4] P. Díaz, Z. González, R. Santamaría, M. Granda, R. Menéndez, C. Blanco,Electrochim. Acta, **168**, 277, (2015).
[5] J. Deng, T. Xiong, F. Xu, M. Li, C. Han, Y. Gong, H. Wang, Y. Wang, Green Chem., **17**,4053 (2015).
[6] H. M. Shiri, A. Ehsani, J. S. Shayeh, RSC Adv.**5**, 91062 (2015).
[7] S. Dhibar, P. Bhattacharya, G. Hatui, D. K. Das,Journal of Alloys and Compounds, **625**, 64 (2015).
[8] M. T. Brumbach, T. M. Alam, P. G. Kotula, B. B. McKenzie, B. C. Bunker,ACS Appl. Mater. Interfaces. **2**, 778 (2014).
[9] X. Yan, X.Tong, J. Wang, C. Gong, M. Zhang, L. Liang, J. Alloys. Compounds, **593**,184, (2014).
[10] Y. Wu,S. Liu, K. Zhao, Z. He, H. Yuan, K. Lv, G. Jia, Ionics.**1**, 11, (2016).
[11] J. Liu, L. Liu, S. Zhuang, X. Wang, F. Tu, **Ionics19**,1255, (2013).
[12] G. Wee, H. Z. Soh, Y. L. Cheah, S. G. Mhaisalkar, M. SrinivasanJ. Mater. Chem., **20**, 6720, (2010).
[13] J. S. Shaikha, R. C. Pawara, R.S. Devan, Y. R. Ma, P. P. Salvi, S. S. Kolekar,P. S.Patil, Electrochimica Acta.,**56**, 2127, (2015).
[14] K.K. Purushothaman, B.Saravanakumar, I.Manoharababu, B. Sethuraman, G. Muralidharan, RSC Advances **4**(45), 23485 (2014).
[15] Y. X. Zhang, M. Kuang, J. J. Wang. CrystEngComm, **16**, 492, (2014).
[16] S.Y. Zhan, C. Z.Wang, K. Nikolowski, H. Ehrenberg, G. Chen, Y. J. Wei. Solid State Ionics **180**, 1198, (2010).
[17] J. H. Kim, S. H. Kang, K. Zhu, J. Y. Kim, N. R. Neale, A. J. Frank, Chem. Commun., **47**, 5214, (2011).
[18] I.Y.Erdogan, O.Gullu.J.Alloy Comp **492**, 378, (2010).
[19] Y.K. Hsu, Y.C. Chen, Y.G. Lin, L.C. Chen, K.H. Chen, Chem. Commun. **21**, 324 (2011).
[20] R. Kumar, P. Rai, A. Sharma. RSC Advances DOI: 10.1039/C5RA20331G, (2015).